Fundamental Behavior of Plates and Stiffened Plates with Welding Imperfections

Yukio UEDA*, Tetsuya YAO**

Abstract

In this paper, the authors describe the results of theoretical and experimental investigations into fundamental behaviors of plates and stiffened plates in compression considering the influences of initial imperfections due to welding. Elastic and elastic-plastic large deflection analyses were performed on nonlinear behaviors to evaluate the compressive ultimate strength of plates and stiffened plates. Buckling analysis was also performed to estimate the influences of welding residual stresses on elastic, elastic-plastic or plastic buckling strength of compressed plates and stiffened plates.

The results of investigation indicate that initial deflection reduces the strength and regidity of compressed plates and stiffened plates. The welding residual stresses also reduce the compressive strength except when a stiffened plate buckles in an overall mode.

KEY WORDS : (Buckling) (Ultimate Strength) (Compressive Strength) (Plate) (Stiffened Plate) (Welding Residual Stress) (Welding Distortion)

1. Introduction

Most of steel strutures are constructed by welding, and the structural elements are accompanied by welding imperfections such as welding residual stresses and distortion. Among many types of structures, a box girder may be one of the typical structures composed of plates and stiffeners. A box girder such as ship's hull or bridge is usually subjected to longitudinal bending, and its deck and bottom plating with longitudinal stiffeners are under inplane compressive and/or tensile load. They play a most important role when longitudinal bending strength of the girder is considered. In general, welding imperfections reduce strength and rigidity of plates and stiffened plates when they are subjected to inplane compressive load. So, an accurate assessment of the influence of welding imperfections on strength and rigidity is necessary to insure the safety of welded structures.

In this paper, the results of fundamental research works, which have been performed by the authors, on buckling and ultimate strengths of plates and stiffened plates subjected to inplane compressive load are summarized, and the influences of welding imperfection are described in the following.

2. Method of Theoretical Analysis

2.1 Typical Behavior of Plates Subjected to Compression

Three stages exist when collapse behavior of a compressed plate is considered.

(1) When a flat plate is loaded by a compressive force, the plate undergoes either elastic, elastic-plastic or plastic buckling with respective stress distributions. This behavior exhibits the simplest geometric nonlinearlity. When stress distribution is elastic-plastic or plastic, the material nonlinearity is also included.

(2) When elastic buckling of a thin plate takes place, the plate can carry an additional load increasing its lateral deflection after buckling. If a plate is initially deflected, lateral deflection of the plate increases from the beginning of loading. To analyze such behavior, the equilibrium condition of the plate against external load should be formulated at the deflected state. This is a typical geometric nonlinear problem.

(3) When the plate in (2) is loaded further, the yielding takes place. After the yielding, plate behavior is characterized as a combined nonlinear behavior of material and geometry. This highly complicated behavior is observed also after elastic-plastic or plastic buckling of thicker plates.

Stiffened plates show fundamentally the same behaviors with those of plates.

2.2 Buckling Analysis

The analysis of buckling strength as a characteristic

† Received on Nov. 8, 1991

* Professor

** Professor Hiroshima University

Transactions of JWRI is published by Welding Research Institute, Osaka University, Ibaraki, Osaka 567, Japan

value was performed based on Energy Theorem applying either Rayleigh-Ritz method or Galerkin's method. Eitherelastic, elastic-plastic or plastic buckling strength was evaluated according to the stress distribution. For the plastic portion of the plate, Deformation Theory of plasticity was applied.

2.3 Elastic Large Deflection Analysis

Elastic large deflection analysis was performed in an analytical manner to simulate the geometrically nonlinear behaviors of plates and stiffened plates. The equilibrium equation was derived based on either Energy Theorem applying Galerkin's method or Principle of Virtual Work. In the analysis of one-sided stiffened plates, the yielding of stiffeners was considered in an approximate manner. Numerical calculation was performed by the incremental method.

2.4 Elastic-plastic Large Deflection Analysis

Elastic-plastic large deflection analysis was performed by the finite element method to simulate combined nonlinear behaviors with respect to geometry and material and to evaluate the ultimate strength of plates and stiffened plates. The incremental equilibrium equation was derived based on Principle of Virtual Work. Flow Theory of Plasticity was applied for the yielded portion.

3. Behavior of Plates Under Compression

3.1 Influence of Welding Residual Stresses on Fundamental Elastic-plastic Behavior of Plates

Firstly, the fundamental elastic-plastic behavior of a plate is examined in tension and/or compression preventing any out-of-plane deformation. The material is assumed to be elastic-perfectly plastic. If a plate is free from welding residual stresses, the average stress-strain relationship is just the same as that of the material, which is shown by solid line in **Fig. 1 (b)**.

Here, a simple distribution of welding residual stresses is assumed in the plate as illustrated in Fig. 1 (a). When a plate is subjected to uniform displacements along the loading edges producing tensile applied stresses, the tensile load is carried only at the portion where compressive residual stresses exist since the side portions are yielded in tension from the beginning of loading. Consequently, the apparent rigidity of the plate is lower than that of the plate free from residual stresses. The average stress-strain relationship for this case is indicated by dashed line, *OBC*, in Fig. 1(b).

When a compressive force is applied to the plate, the average stress-strain relationship is the same as that of the plate free from residual stresses until the yielding takes

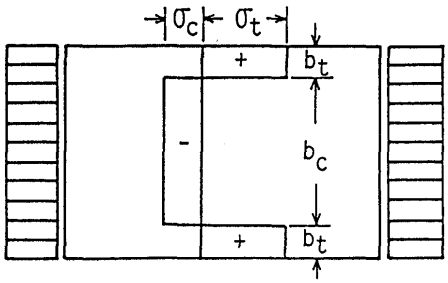

(a) Simplified residual stress distribution

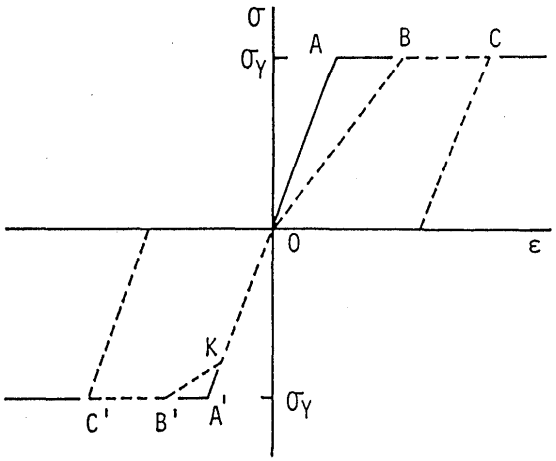

(b) Average stress-strain relationship

Fig. 1 In-plane rigidity of plate containing welding residual stresses under uni-axial load

place at the portion where compressive residual stresses exist. After this yielding, compressive load increments are carried only at the side portions where residual stresses are in tension, and the in-plane rigidity is largely reduced. The average stress-strain relationship for this case is given by the dashed line, *OKB'C'*, in Fig. 1(b).

In both cases of compressive and tensile loading, the maximum load is the same regardless of the welding residual stresses as far as the welding residual stresses are self-equilibrating in the plate.

When the plate is unloaded at point *C* or *C'*, the relationship takes the path indicated by dashed line with a narrow in Fig. 1(b), which is parallel to the loading path indicated by the solid line. After unloading, the plate becomes free from residual stresses. This is the basic idea behind mechanical stress relieving.

3.2 Influence of Welding Residual Stresses on Buckling Strength[1-3)]

For a simplified distribution of welding residual stresses, buckling strength of an infinite strip was evaluated[1)], and the results are shown in **Fig. 2(a)**. The buckling strength in the figure indicates the minimum

critical load. The wave length of the buckling mode is very close to the plate breadth.

In order to verify the accuracy of the theoretical results, experiments on local buckling of columns with square section were carried out applying an axial compressive force[2]. Both theoretical and experimental results showed good correlation as presented in Fig. 2(b).

Influences of welding residual stresses on local buckling strength of web and flange in built-up I-section column under axial compression were also estimated in Ref. 3).

3.3 Fundamental Behavior and Ultimate Strength of Square Plate[4,5]

A series of elastic-plastic large deflection analysis was performed on simply supported square plates subjected to compression to investigate into the influences of initial deflection and welding residual stresses on plate behavior[4]. In the analysis, the loading edges were kept to be straight, while the edges parallel to the load were assumed to move and deform freely in the original plane to compare the calculated results with experimental ones.

Calculated load-deflection and load-displacement relationships are plotted in **Fig. 3** and **4**, respectively. The solid curves represent the results consults considering only the initial deflection, and the dashed curves containing both the welding residual stresses and initial deflection. The welding residual stresses were produced by giving inherent strain increments at the portion where tensile residual stresses exist.

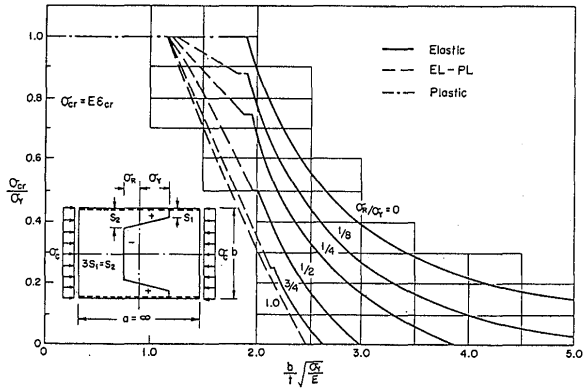

(a) Buckling strength of infinite strips simply supported along opposite sides (Theory)

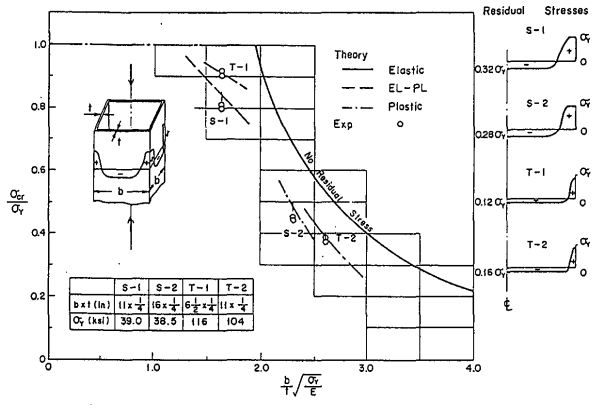

(b) Local buckling strength of built-up colums with square cross section (Theory and experiment)

Fig. 2 Buckling strength of plate in compression

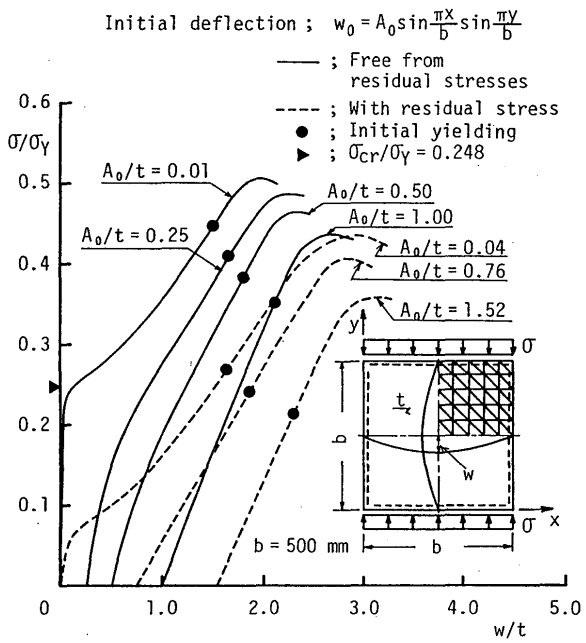

(a) t=4.5mm

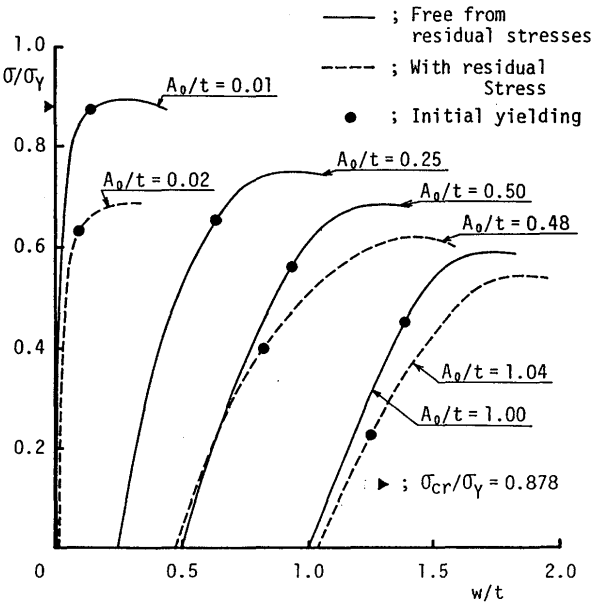

(b) t=9.0mm

Fig. 3 Average stress-central deflection curves for square plates under compression

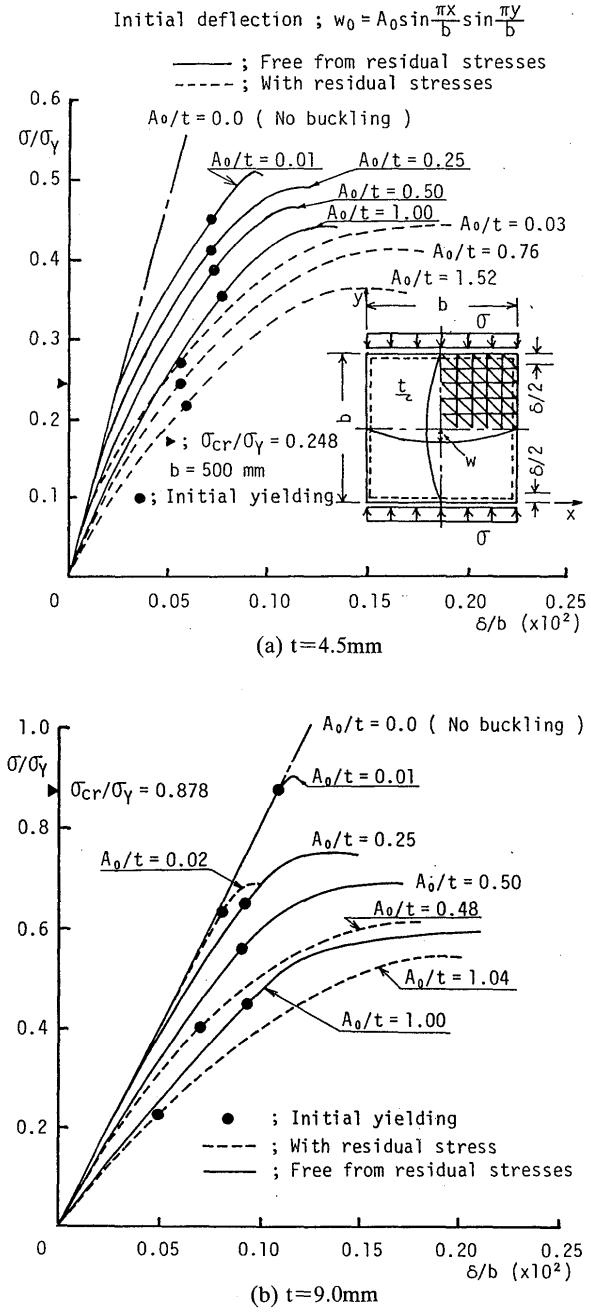

Fig. 4 Average stress-displacement curves for square plates under compression

The evaluated ultimate strengths are plotted in **Fig. 5** comparing with the experimental results. Some differences are observed between the theoretical and experimental results for thinner plates. This may be attributed to the difficulty to get simply supported condition in experiments. However, taking into account of the sensitive nature of the plate behavior, it may be said that the both results coincide well with each other for all cases.

Influences of the shape of initial deflection, initial stresses accompanying with initial deflection and the pattern of residual stress distribution on behavior of plates were also discussed in Refs. 4) and 5).

3.4 Fundamental Behavior and Ultimate Strength of Rectangular Plate[8-13]

3.4.1 Initial Deflection and Welding Residual Stresses.

A plate element from a stiffened plate assemblage was considered in the analyses. The plate has an initial deflection and welding residual stresses, as illustrated in **Fig. 6**. To represent the assemblage continuity, the plate was assumed to be simply supported and remain straight along all edges while subjected to in-plane movements.

Many measurements of the maximum magnitude of initial deflection have been carried out on various locations in ship structures, and some quality standards

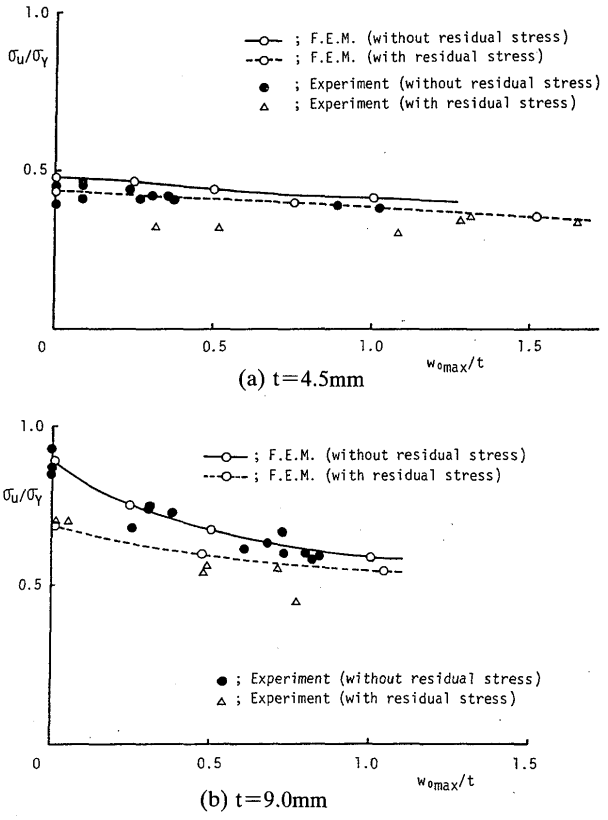

Fig. 5 Influence of initial deflection due to welding on compressive ultimate strength of square plates

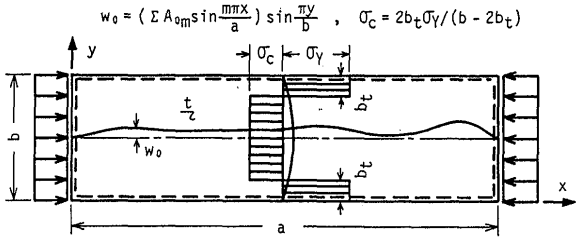

Fig. 6 Long rectangular plate with welding residual stresses and initial deflection

including limitations of the maximum initial deflections were published[6,7] based on the measured results. Few measurements, however, have been carried out as to the mode of initial deflection. In Refs. 11) and 13), a series of measurements on the mode of initial deflection was carried out on 33 panels of the deck plates of a bulk carrier and a pure car carrier. The aspect ratio, a/b, of the measured panel was between 2.65 and 4.41, and the breadth-to-thickness ratio, b/t, between 23.19 and 97.5.

The initial deflection was approximated in the following form:

$$w_0 = \left(\Sigma A_{om} sin\frac{m\pi x}{a}\right) sin\frac{\pi y}{b} \qquad (1)$$

The coefficients, A_{om}, up to $m = 11$ were calculated based on the measured data along the center line, $y=b/2$, of the panel applying the method of least squares. They are summarized in **Table 1**.

It should be pointed out that the one half-wave component is the largest and the coefficients of odd terms are greater than those of even terms in most cases. This results in the so-called hungry-horse mode of initial deflection.

The residual stresss in the plate are produced by fillet weld of the stiffeners along the edges $y = 0$ and $y = b$. Their distribution was assumed to be rectangular as shown in Fig. 6, which may be valid when a continuity condition between the plate elements of the stiffened plating is considered. If the residual stresses are assumed to be self-equilibrating only in the individual plate, there exists the following relationship between the compressive residual stress, σ_c, and the tensile residual stress, σ_t.

$$2b_t\sigma_t=(b-2b_t)\,\sigma_c \qquad (2)$$

where b_t represents the breadth where the tensile residual stresses are acting.

3.4.2 Rectangular Plate with Simple Initial Deflection.

Series of elastic-plastic large deflection analyses by the finite element method were performed on rectangular plates with initial deflection[8,9,13]. Although the measured mode of initial deflection was complex, an initial deflection of a simple mode was firstly assumed as:

$$w_0=\left(A_{01}sin\frac{\pi x}{a}+A_{02}sin\frac{2\pi x}{a}\right)sin\frac{\pi y}{b} \qquad (3)$$

The breadth and thickness of the plate were taken as 1,000mm and 12mm, respectively, and the yield stress of the material as 28kgf/mm^2. Welding residual stresses were not considered in this analysis.

The evaluated ultimate strengths changing the aspect ratio of the plate between 0.25 and 2.0 are plotted in

Table 1 Coefficients of deflection components of measured initial deflection

(Bulk Carrier) (in mm)

No.	a×b×t	w_{0max}	A_{01}	A_{02}	A_{03}	A_{04}	A_{05}	A_{06}	A_{07}	A_{08}	A_{09}	A_{010}	A_{011}
1	2400x800x34.5	-1.320	-1.346	-0.090	-0.224	-0.036	-0.087	-0.082	0.102	-0.036	-0.014	0.026	-0.028
2	2400x800x34.5	-0.770	-0.746	-0.026	-0.124	0.001	-0.066	-0.023	0.112	0.016	0.016	0.065	-0.008
3	2400x800x34.5	-1.550	-1.235	-0.339	-0.344	0.129	-0.061	-0.015	-0.031	-0.031	-0.033	0.075	-0.018
4	2400x800x34.5	-1.260	-1.247	0.178	-0.090	-0.002	-0.004	0.034	0.023	0.018	0.029	0.009	0.023
5	2400x800x34.5	-1.040	-0.968	-0.176	-0.133	-0.052	0.043	-0.020	0.030	0.007	-0.000	-0.000	0.030
6	2400x800x34.5	-1.090	-1.136	-0.107	-0.102	-0.007	0.012	-0.014	0.015	-0.011	-0.039	-0.004	-0.006
7	2400x800x34.5	-0.590	-0.563	-0.021	-0.179	-0.044	-0.014	-0.039	-0.009	0.011	0.020	-0.043	0.042
8	2400x800x34.5	-1.330	-1.101	-0.481	-0.102	-0.032	-0.020	-0.043	0.032	0.025	0.036	-0.014	0.019
9	2400x800x34.5	-1.680	-1.239	0.483	-0.268	0.050	0.029	-0.029	-0.046	0.110	0.056	0.004	-0.008
10	2400x800x34.5	-1.420	-1.339	-0.094	-0.090	-0.024	-0.176	-0.040	-0.049	-0.027	-0.050	0.009	-0.031
11	2400x800x34.5	-1.210	-1.158	-0.142	-0.091	-0.059	-0.057	-0.062	-0.055	0.038	-0.015	-0.022	-0.035
12	2400x800x34.5	-1.390	-1.481	0.024	-0.283	-0.028	-0.062	-0.013	-0.047	0.003	-0.032	-0.019	-0.022
13	2800x800x15	-2.390	-2.668	0.286	-0.686	0.097	-0.534	-0.008	-0.234	0.058	-0.105	0.044	-0.073
14	2800x800x15	-4.150	-4.535	-0.183	-1.419	0.387	-0.656	0.138	-0.341	0.043	-0.155	0.092	-0.135
15	2800x800x15	-3.740	-3.955	-0.218	-1.204	-0.095	-0.359	-0.025	0.023	-0.080	0.137	0.016	0.015
16	2800x800x19	-3.180	-3.339	-0.188	-0.297	0.059	-0.194	0.128	-0.143	0.030	-0.070	0.014	-0.042
17	2800x800x19	-3.680	-4.187	0.441	-0.867	0.150	-0.388	-0.110	-0.181	-0.045	-0.035	-0.037	-0.074
18	2800x800x19	-3.810	-4.161	0.434	-0.921	-0.013	-0.559	-0.015	-0.243	0.004	-0.083	-0.022	-0.093
19	2100x800x19	-3.010	-3.092	0.336	-0.362	0.056	0.017	0.076	-0.010	0.058	0.060	0.030	-0.013
20	2100x800x19	-3.360	-3.687	-0.049	-0.749	-0.055	-0.382	-0.016	-0.142	0.048	0.041	-0.013	-0.092
21	2100x800x19	-3.110	-3.634	-0.035	-0.937	0.043	-0.336	0.069	-0.078	0.119	0.069	0.027	-0.046

(Car Carrier)

No.	a×b×t	w_{0max}	A_{01}	A_{02}	A_{03}	A_{04}	A_{05}	A_{06}	A_{07}	A_{08}	A_{09}	A_{010}	A_{011}
1	3440x780x11	-5.290	-5.949	-0.223	-1.936	-0.070	-0.598	-0.148	-0.455	0.031	0.020	0.022	0.008
2	3440x780x11	-5.360	-5.611	0.735	-1.948	-0.075	-0.793	0.075	-0.547	0.116	-0.030	0.013	-0.030
3	3440x780x11	-4.620	-4.643	0.702	-1.456	-0.147	-1.065	-0.073	-0.362	0.146	0.128	0.057	0.083
4	3440x780x11	-5.870	-3.425	-1.500	-2.965	0.525	-0.966	-0.380	-0.332	0.124	-0.125	-0.026	0.005
5	3440x780x11	-5.470	-5.125	0.586	-1.832	0.318	-0.945	0.107	-0.629	-0.013	-0.082	-0.064	-0.057
6	3440x780x11	-5.650	-5.647	0.133	-2.167	0.147	-1.201	0.209	-0.270	0.114	-0.006	0.051	-0.003
7	3440x780x8	-3.970	-2.635	-1.455	-0.871	0.328	0.349	0.194	0.154	0.027	0.114	0.074	0.108
8	3440x780x8	1.300	0.605	-0.508	0.037	-0.308	-0.349	0.082	0.058	-0.058	-0.107	0.002	0.014
9	3440x780x8	2.330	0.269	-0.198	-1.195	0.621	0.144	-0.350	-0.085	0.029	-0.066	0.006	-0.080
10	3440x780x8	1.510	-0.142	0.720	0.482	0.012	0.261	0.073	0.158	0.086	0.120	0.006	-0.014
11	3440x780x8	-1.350	-0.497	-0.338	0.339	-0.159	0.200	-0.252	0.154	-0.032	0.031	-0.120	0.017
12	3440x780x8	-2.960	0.460	1.023	-0.981	0.259	-0.862	0.100	-0.156	0.096	0.032	0.023	0.076

Fig. 7. It is well known that the buckling strength of a simply supported long plate under uni-axial compression is a minimum the aspect ratio being an appropriate integer. However, Fig. 7 indicates that the ultimate strength assuming an uni-modal initial deflection ($A_{01}/t=0$ or $A_{02}/t=0$) is not necessarily a minimum for these aspect ratios. The smallest aspect ratio giving the minimum ultimate strength was appoximately 0.7 for the size of plate shown in Fig. 7 when initial deflection is small.

In case of $A_{01}/t = A_{02}/t = 0.01$, the ultimate strength suddenly decreased when aspect ratio changes from 1.36 to 1.38. The result indicates the possibility of sudden change of ultimate strength with respect to aspect ratio.

For the plate with aspect ratio of 1.25, two kinds of shape and magnitude of initial deflection were used, which were $A_{01}/t=A_{02}/t=0.1$ and $A_{01}/t=0.5$, $A_{02}/t=0.1$. Although the second plate has a larger initial deflection, its ultimate strength was higher than the first as indicated in Fig. 7. In the first case, the plate deflects and collapses in two half-waves in the loading direction, while in the second case, it collapses in one half-wave. The selection of the stable deflection mode depends on the magnitude of the components of the initial deflection and their ratios. This ratio is defined as the critical ratio of the components of initial deflection[8,9,13].

For longer plates with uni-modal initial deflection, whose mode is the same as that of the buckling mode, the ultimate strengths were estimated based on the results in Fig. 7. The estimated ultimate strengths are plotted in **Fig. 8**. If the deflection mode is stable up to collapse, the ultimate strength curves are represented by bold solid and chain lines. The abrupt changes are observed in the ultimate strength curves at the aspect ratio of $\sqrt{m(m+1)}$, where the buckling mode changes from m half-waves to $(m+1)$ half-waves in the loading direction.

Also for longer plates with uni-modal initial deflection, whose mode is not necessarily the same with that of the buckling mode corresponding to the aspect ratio, the ultimate strength was estimated. The results are shown in **Fig. 9**. The lowest ultimate strength is almost constant for a specified magnitude of initial deflection, irrespective of the aspect ratio.

3.4.3 Minimum Ultimate Strength.

A series of elastic-plastic large deflection analysis was performed to derive formulae for the minimum ultimate strengths, which are the lowest ultimate strengths in Fig. 9 for specified magnitudes of initial deflection[10,13]. In the analysis, the aspect ratio of the plate was changed between 0.4 and 1.0 keeping its breadth and the yield stress as constants to get the minimum ultimate strengths for various thicknesses. The magnitude of uni-model initial deflection was taken as 0.01, 0.1, 0.2, 0.3, 0.4 and 0.5 times the thickness. The calculated minimum ultimate strengths are plotted against the non-dimensionalized paramener, $(b/t)\sqrt{\sigma_Y/E}$, in **Figs. 10** (a), (b) and (c), in which the magnitude of welding residual stresses varies, $2b_t/b$ being 0.0, 0.1 and 0.2, respectively.

In these figures, the minimum ultimate strengths are

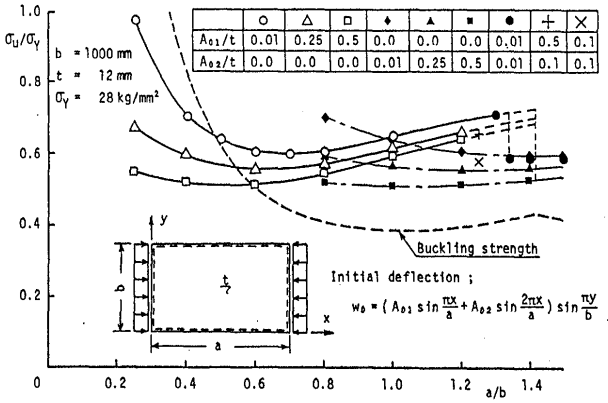

	○	△	□	♦	▲	■	●	+	×
A_{01}/t	0.01	0.25	0.5	0.0	0.0	0.0	0.01	0.5	0.1
A_{02}/t	0.0	0.0	0.0	0.01	0.25	0.5	0.01	0.1	0.1

Fig. 7 Compressive ultimate strength of short rectangular plate with simple initial deflection

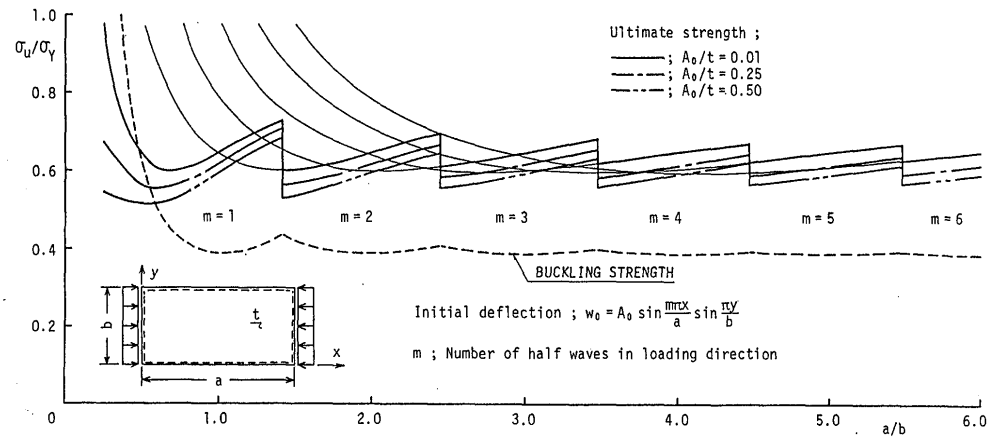

Fig. 8 Compressive ultimate strength of long rectangular plate with uni-model initial deflection

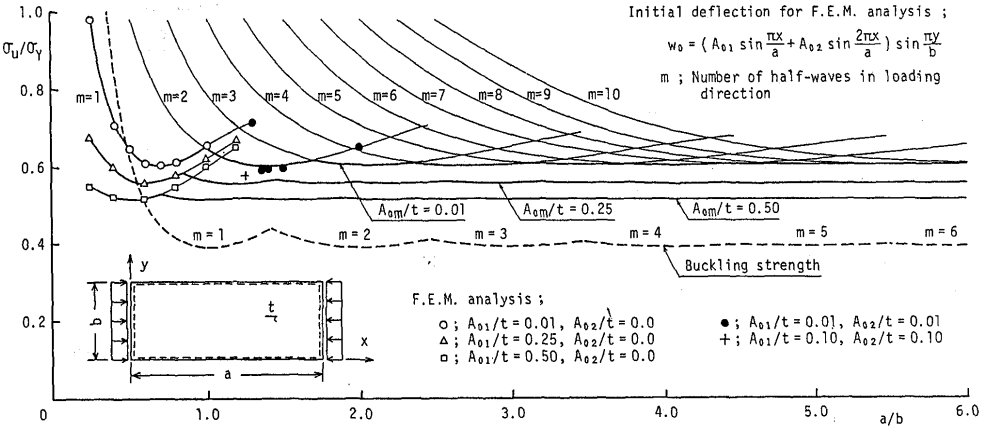

Fig. 9 Compressive ultimate strength of long rectangular plate with uni-model initial deflection

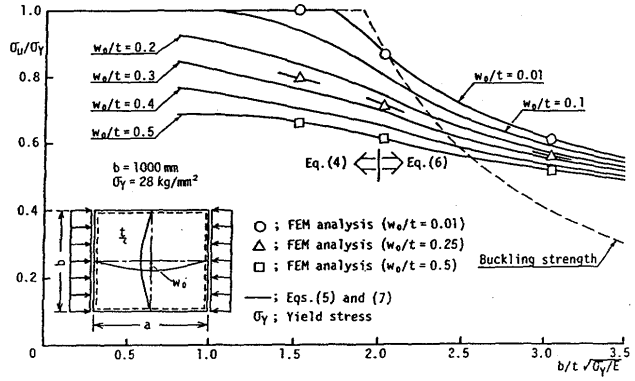

(a) Rectangular plate free from residual stresses

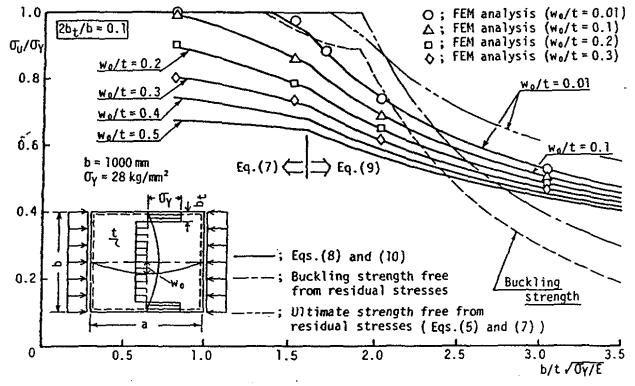

(b) Rectangular plate with residual stresses ($2b_f/b=0.1$)

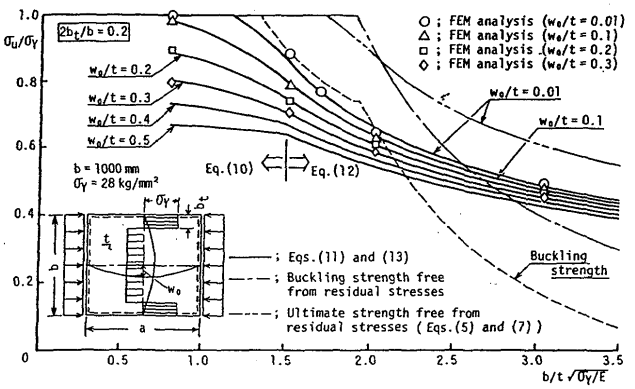

(c) Rectangular plate with residual stresses ($2b_f/b=0.2$)

Fig.10 Minimum compressive ultimate strength of rectangular plates

represented by solid lines. They are expressed by the following simple formulae, which were derived by applying the method of least squares to the calculated values.

(a) $2b_f/b=0.0$

(i) $0.8 \leqq \xi \leqq 2.0$

$$\sigma_u/\sigma_Y=(-2.431\eta^2+1.6826\eta-0.2961)(\xi^2-4.0)+(7.2745^2-4.7431\eta+0.6709)(\xi-2.0)+Z_1 \quad (4)$$

$$Z_1=(-0.3579\eta^2+0.1748\eta+0.8598)/(2.2432\eta+1.3322)+0.0373\eta+0.2481 \quad (5)$$

(ii) $2.0 < \xi \leqq 3.5$

$$\sigma_u/\sigma_Y=(-0.3597\eta^2+0.1748\eta+0.8598)/(\xi+2.2432\eta-0.6678)+0.0373\eta+0.2481 \quad (6)$$

(b) $2b_f/b=0.1$

(i) $0.8 \leqq \xi \leqq 1.6$

$$\sigma_u/\sigma_Y=(-0.398\eta^2+0.4339\eta-0.1342)(\xi^2-2.56)+(1.0814\eta^2-0.7551\eta+0.1020)(\xi-1.6)+Z_2 \quad (7)$$

$$Z_2=(0.4974\eta^2+0.8281\eta+1.0171)/(2.7942\eta+1.2908)-0.1849\eta+0.1571 \quad (8)$$

(ii) $1.6 < \xi \leqq 3.5$

$$\sigma_u/\sigma_Y=(0.4974\eta^2+0.8281\eta+1.0171)/(\xi+2.7942\eta-0.3092)-0.1849\eta+0.1571 \quad (9)$$

(c) $2b_f/b=0.2$

(i) $0.8 \leqq \xi \leqq 1.5$

$$\sigma_u/\sigma_Y=(-0.3317\eta^2+0.6314\eta-0.2656)(\xi^2-2.25)+(0.5369\eta^2-0.7798\eta+0.2854)(\xi-1.5)+Z_3 \quad (10)$$

$$Z_3=(0.292\eta^2+1.2936\eta+0.7471)/(2.897\eta+1.1189)-0.2715\eta+0.2057 \quad (11)$$

(ii) $1.5 < \xi \leqq 3.5$

$$\sigma_u/\sigma_Y=(0.292\eta^2+1.2936\eta+0.7471)/(\xi+2.897\eta-0.3811)-0.2715\eta+0.2057 \quad (12)$$

where

$$\xi = (b/t)\sqrt{\sigma_Y/E},\quad \eta = A_0/t$$

The ultimate strengths calculated by these equations are the conservative ones.

3.4.4 Fundamental Behavior of Rectangular Plate with Complex Initial Deflection.

An elastic large deflection analysis was performed on no.6 panel of the car carrier in Table 1, which may be one of the common modes of initial deflection[11,13]. The welding residual stresses were not considered in this analysis. Based on the calculated nodal displacements of the finite elements along the center line, the deflection was approximated by the trigonometric series as:

$$w=\left(\Sigma A_m \sin\frac{m\pi x}{a}\right)\sin\frac{\pi y}{b} \qquad (13)$$

The calculated relationships between average compressive stress and deflection components are represented by dashed lines in **Fig. 11** (a). The stress is non-dimensionalized by the elastic buckling stress, and the deflection components by the thickness. Figure 11(b) shows changes of the modes of deflection and curvature along the center line of the plate.

All component modes of the initial deflection increase until the load approaches the buckling one, but all except the five half-wave mode diminish above the buckling load. In this case, the five half-wave mode becomes stable, though the aspect ratio of this plate is 4.41, and the buckling mode is four half-waves in the loading direction. It was known that the stable deflection mode of an initially deflected plate above the buckling load is often higher than the buckling mode by one or two degrees, depending on the mode and the magnitude of initial deflection[8-13].

For the same panel, elastic-plastic large deflection analysis was performed taking the yield stress as 28kgf/mm^2. The breadth and length of the plate were kept

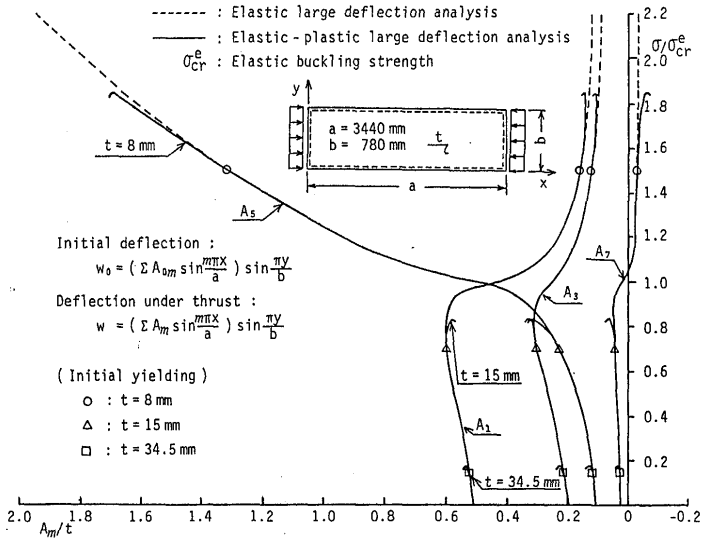

(a) Relationships between average stress and deflection components

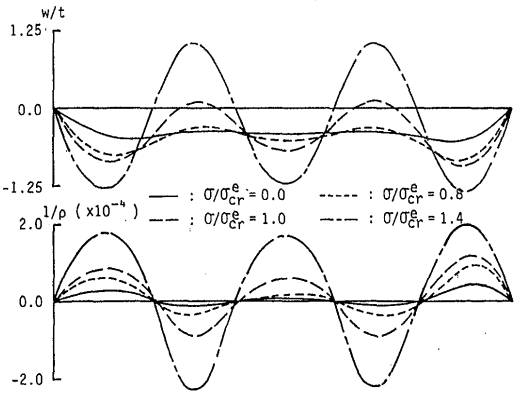

(b) Change of deflection and and curvature

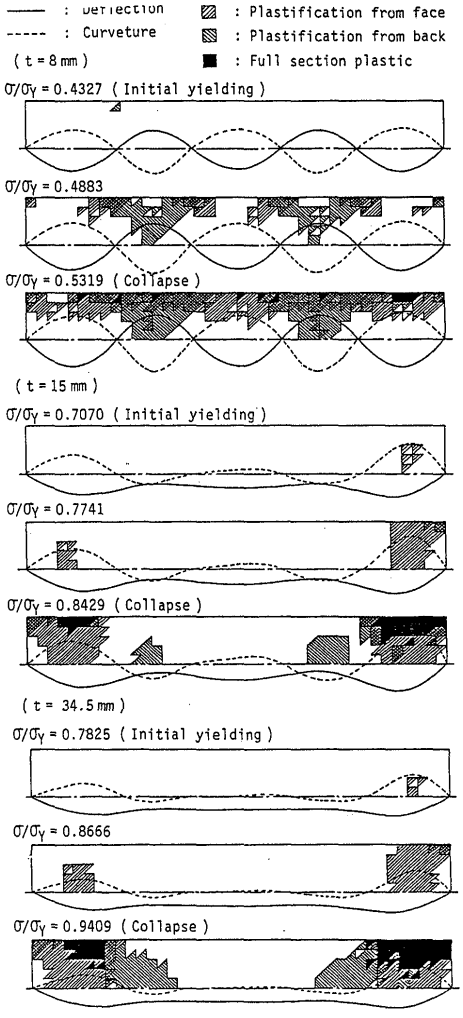

(c) Spread of plastic zone

Fig.11 Deflection and plastification of long rectangular plate with complex initial deflection under compression

the same, but its thickness was changed as 8 mm, 15 mm and 34.5 mm in the analysis. The results of calculation are illustrated by solid lines in Fig. 11 (a), and the spread of plastic zone in Fig. 11(c).

In the case of a thin plate of 8mm thickness, the compressive stress does not increase in the central portion of the plate when deflection becomes large above the buckling load. Consequently, the compressive load is carried mainly near the supporting edges, $y=0$ and $y=b$, where the deflection is small. For further load increments, the deflection mode is stable and initial yielding takes place at the supporting edges. The plastic zone spreads as the load increases, and the plate finally collapses when plastic zone has spread along the edges. The entire magnitude of initial deflection does not influence the ultimate strength, but only the magnitude of component mode corresponding to the stable deflection does.

In contrast, in the case of a thick plate of 34.5 mm thickness, initial yielding takes place at a certain point along the center line. At this load, as the deflection is small, the mode is almost the same as that of the initial deflection, and the effect of large deflection is not apparent. Therefore, the in-plane stress is almost the same all over the plate, though the bending stress varies depending on the curvature. Consequently, initial yielding takes place at the point where the maximum bending stress (i.e. the maximum curvature) is produced. This point is usually located along the center line of the plate just near the point where the curvature of the initial deflection is a maximum. For further increases of load, the plastic zone spreads from the center line, and the compressive load is not carried in this zone. Consequently, the additional compressive load is carried near the supporting edges, and the plate finally collapses when the portions near the edges become fully plastic. In this case, the deflection mode and the location of the maximum curvature at collapse are almost the same as those for the initial deflection. Accordingly, the ultimate strength is dependent on the maximum curvature of the initial deflection but its maximum magnitude.

In the case of a plate with a medium thickness of 15mm, initial yielding takes place at a certain point along the center line during the course of a mode changing from initial to stable mode. Although the fundamental behavior is almost the same as for the thick plate, this interaction between the component modes may accelerate or decelerate the spread of plastic zone and this greatly influences the resulting ultimate strength.

3.4.5 Prediction of Ultimate Strength of Rectangular Plate with Multi-modal Initial Deflection.

Based on the results in 3.3.4, simple method was proposed to predict the ultimate strength of rectangular plates with welding residual stresses and complex initial deflection in Refs. 11), 12) and 13). For thin plates, Deflection Method was proposed, in which the attention was focussed on the component mode of initial deflection that becomes stable above the buckling load. For thick plates, Curvature Method was proposed paying attention to the maximum curvature of initial deflection. Good predictions were made applying these method.

The methods to predict initial deflection and welding residual stresses, as well as the compressive ultimate strength of a deck plate, were also proposed in Ref. 12) when the sizes of plates and stiffeners and the welding conditions were given.

4. Behavior of Stiffened Plate under Compression

4.1 Buckling Strength[15,16]

When stiffeners are fitted to a plate by welding, residual stresses are produced both in the plate and the stiffener. In order to know the fundamental feature of a stiffened plate and the influences of welding residual stresses on buckling strength of a stiffened plate under uni-axial compression, a simple model was considered in Ref. 15). The model was a square plate with a both-sided stiffener fitted along the center line in loading direction, which was symmetric with respect to the middle plane of the plate. This model is shown in **Fig. 12**. To know the distribution of welding residual stresses in this simple stiffened plate, the steel models were constructed by staggered intermitted fillet welds. The welding residual stresses were measured by applying the sectioning method. The distribution of measured residual stresses could be approximated with straight lines as indicated in Fig. 12. With this distribution, theoretical analysis was

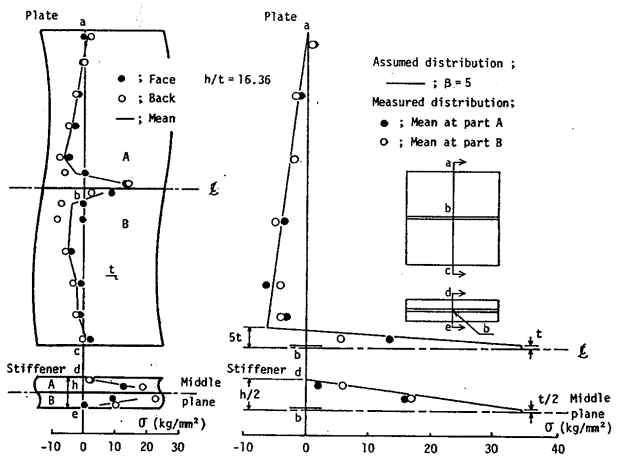

(a) Measured distribution (b) Comparison of measured and idealized distributions

Fig.12 Distribution of welding residual stresses in both-sided stiffened plate

performed changing the parameter, β, and the magnitude of flexural rigidity of the stiffener[15,18-20]. The calculated buckling strengths are plotted in **Fig. 13**.

The stiffness ratio of the flexural rigidity of a stiffener to that of a plate, γ, plays an important role when the buckling of a stiffened plate is considered. If γ is smaller than γ^{B}_{min}, the primary buckling takes place in an overall mode. Then, with further increases in load, the secondary buckling in a local mode takes place. Constray to this, primary buckling in a local mode firstly takes place, and then the secondary buckling in an overall mode when γ is greater than γ^{B}_{min}.

The welding residual stresses increase the overall buckling strength, since tensile residual stresses exist in the central portion where deflection is produced by buckling, whereas they decrease the local buckling strength because the compressive residual stresses exist in the central portion of the plate panels. It is known from Fig. 13 that the minimum stiffness ratio, γ^{B}_{min}, which is defined as the stiffness ratio at the intersecting points of local and overall buckling strength curves, decreases with the increases in welding residual stresses.

Buckling strength of one-sided stiffened plate was also discussed in Ref. 16). In this case, load eccentricity of loading is induced after the primary buckling, and the secondary buckling does not take place in a strict sense. The buckling strength in an overall mode was derived, which is given by Eq. (15) in 4.2.2.

4.2 Fundamental Behavior and Ultimate Strength[14-20]

4.2.1 Post Buckling Behavior and Ultimate Strength of Both-sided Stiffened Plate.

A series of elastic-plastic large deflection analysis was performed on a simplest stiffened plate shown in **Fig. 14** to know the fundamental behavior of stiffened plates in compression[14,18-20]. The initial deflection of the following form was assumed.

$$w_o = A_o \sin\frac{\pi x}{b}\sin\frac{\pi y}{b} + B_o \sin\frac{2\pi x}{b}\sin\frac{2\pi y}{b} \qquad (14)$$

The welding residual stresses were not considered in this analysis.

For some typical cases, calculated load-deflection curves are shown in Fig. 14. The evaluated ultimate strengths are plotted in **Fig. 15** against the hight of the stiffener, where *U1-U7* represents the ultimate strength of a stiffened plate with small initial deflection ($A_o/t = B_o/t = 0.01$), and *UD1-UD4* represents that with large initial deflection ($A_o/t = B_o/t = 0.5$).

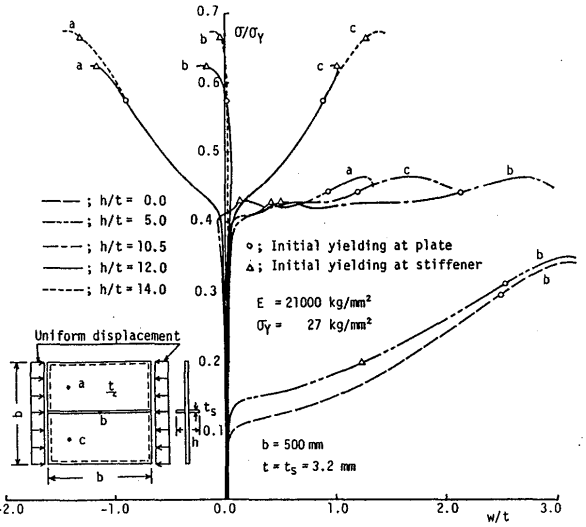

Fig.14 Average stress-deflection curves for symmetrically both-sided stiffened plate under compression

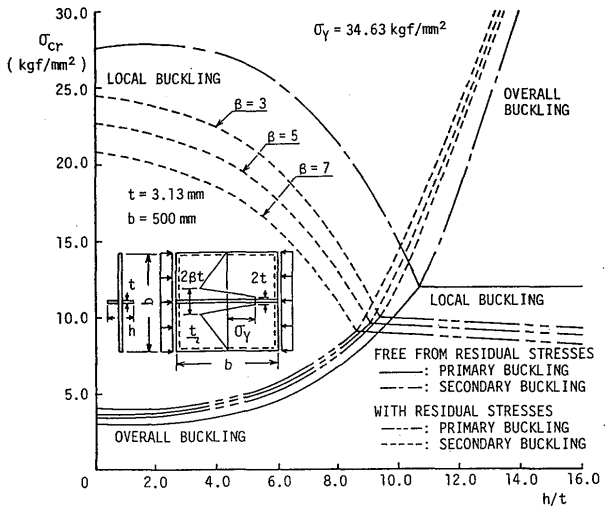

Fig.13 Compressive buckling strength symmerically both-sided stiffened plates

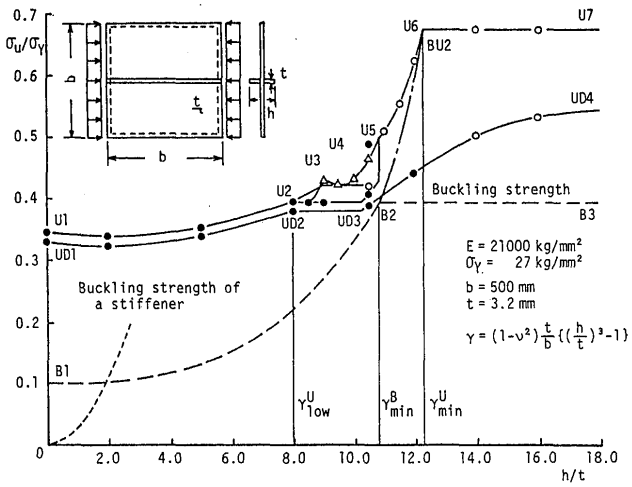

Fig.15 Ultimate strength and minimum stiffness ratio of symmetrically both-sided stiffened plates under compression

The behavior of the stiffened plate with small initial deflection varies depending on the stiffness ratio of a stiffener to a plate as follows.

(a) *U1-U2*

The ultimate strength for a stiffened plate with small stiffness ratio ($h/t < 4$) is approximately constant, and it gradually increases with increase in stiffness ratio ($h/t > 4$). It stops increasing and shows the local maximum at point *U2*. For a smaller stiffness ratio in this range, the initial yielding occurs firstly in the plate and the yielding of the stiffener follows. Contrary to this, the order of initial yielding is reversed for larger value of the stiffness ratio. However, regardless of the order of initial yielding, the stiffened plate collapses in an overall mode in this range of the stiffness ratio.

The stiffness ratio, γ, calculated from h/t at point *U2* was defined as γ^{U}_{low}, which gives the local maximum of the compressive ultimate strength. The presence of the local maximum is due to the rapid spread of the plastic zone in the stiffener.

(b) *U2-U5*

In this range, the stiffened plate shows a very complicated behavior. when $h/t=9.5$, there exist two peak points in the load-deflection curves as indicated in Fig. 14. The load at these two peak points are plotted by △ and ○ in Fig. 15. The first peak is due to the yielding of the stiffener, and the second peak that of the plate. In this range of the stiffness ratio, the collapse was still in overall mode. The collapse mode in the range *U1-U5* was defined as Mode *OO*, which implies overall collapse after overall buckling.

(c) *U5-U6*

Between *U5* and *U6*, the stiffness ratio is greater than γ^{B}_{min}. Therefore, the local buckling of the plate firstly takes place, and the overall buckling as a stiffened plate follows, when there exists no initial deflection. When initial deflection is small, the deflection of the stiffener increases rapidly as the load approaches to the secondary buckling strength, and the yielding of the stiffener takes place. This yielding accelerates the deflection in an overall mode, and the stiffened plate can carry no more load. For this reason, the ultimate strength of a stiffened plate with this range of h/t ratio is very close to the secondary buckling strength in an overall mode when the initial deflection is zero or very small. The collapse mode in this range was defined as Mode *LO*, which means overall collapse after local buckling.

(d) *U6-U7*

In this range, the plate collapses locally after its local buckling, before the secondary buckling in an overall mode takes place. The ultimate strength is almost constant regardless of the stiffness ratio of the stiffener to the plate. This constant value may be regarded as the maximum limiting value of the compressive ultimate strength of a stiffened plate. The stiffness ratio calculated with h/t at point *U6* was defined as the minimum stiffness ratio, γ^{U}_{min}, against the ultimate strength of a stiffened plate, which guarantees the maximum ultimate strength. The collapse in this range was defined as Mode LL, which indicates local collapse after local buckling.

As is known from Fig. 15, the initial deflection largely reduce the compressive ultimate strength of a stiffened plate when it collapses in Mode *LO*. In contrast, the decrease in the ultimate strength is not so much when Mode *LL* collapse takes place. The stiffness ratio that the collapse mode changes from *LO* to *LL* is defined as the "effective minimum stiffness ratio", ${}_{eff}\gamma\, U_{min}$, against the ultimate strength of a stiffened plate with initial deflection.

A series of experiments was carried out to investigate into the influences of initial deflection and welding residual stresses on compressive ultimate strength of both-sided stiffened plates[15]. The hight of a stiffener was chosen so that collapses in Mode *LO* and Mode *LL* occur. Regarding the influence of initial deflection, the same tendency was observed as indicated in Fig. 15. As for the influence of welding residual stresses, the ultimate strength was greatly reduced when Mode *LL* collapse took place, whereas increased for Mode *LO* collapse[15].

4.2.2 Post Buckling Behavior and Ultimate Strength of One-sided Stiffened plate.

The analytical method to predict the ultimate strength of a stiffened plate with one-sided stiffeners shown in **Fig. 16** was also developed considering both welding residual stresses and initial deflection. The *N* stiffeners of the same size are fitted to the plate at an equal spacing. In this method, the influence of the yielding of stiffeners was considered in an approximate manner[16,18-20].

Firstly, a square plate with one stiffener is considered without welding residual stresses. **Figure 17** shows the load-deflection relationships obtained by the proposed method together with those by the elastic-plastic large deflection FEM analyses[16].

As in the case of a symmetrically both-sided stiffened plate, there exist three typical collapse modes depending of the stiffness ratio of the stiffener to the plate, which

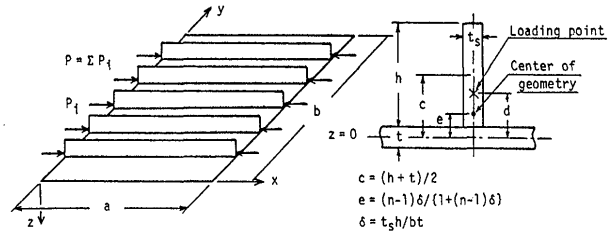

Fig.16 One-sided stiffened plate

are:

(a) *Mode OO (h/t=5.0)*

When the stiffness ratio is small, yielding of the stiffener (P_s) is observed first. A stiffend plate can carry further load, and the yielding of the plate (P_p) takes place at point a on the supporting edge of the plate. The initial yielding of the plate was regarded as the ultimate strength for this case.

(b) *Mode LO (h/t=6.25 and 6.5)*

For the case of intermediate stiffness ratio, local buckling of the plate proceeds. Consequently, the rigidity of the plate decreasses and load applied originally at the center of geometry of the section becomes eccentrical. Then, the deflection of the stiffener increases rapidly, and yielding takes place in the stiffener. Soon after the yielding of the stiffener, the load shows a local maximum (P_l), and becomes to decrease as the deflection increases. However, the stiffened plate again carry the load increment. Then, plate yielding takes place between points *a* and *b* along the supporting edge (P_p). In this case, the higher load between P_l and P_p was regarded as the ultimate strength of a stiffened plate.

(c) *Mode LL (h/t>6.75)*

When the stiffness ratio becomes larger, local buckling of the plate occurs, and then yielding of the plate takes place at point *b* (P_p) before the load shows a local maximum due to the yielding of a stiffener. This load was regarded as the ultimate strength in this case.

The ultimate strengths predicted by the approximate method are plotted in **Fig. 18** together with those by FEM analysis[16]. Two loading conditions were considered. In one case, load was applied at the center of geometry of the section, and the other at the middle plane of the plate. The predicted results showed good correlations with those by FEM analysis. The collapse mode changes from Modes *OO* to *LO* and from *LO* to *LL* at two points indicated by × on solid lines. At these points, P_l is equal to P_p.

Figure 19 shows the influence of initial deflection on the ultimate strength of a one-sided stiffened plate[16,18-20]. The ultimate strength is reduced according to the magnitude of initial deflection. When initial deflection is small, the minimum stiffness ratio, γ^U_{min}, can be determined as the stiffness ratio which terminates the collapse mode from *LO* to *LL*. This stiffness ratio corresponds to that at the higher point of two × in Fig. 18. When initial deflection is large or the load is applied eccentrically, the effective minimum stiffness ratio, $_{eff}\gamma^U_{min}$, can be determined in the similar way as γ^U_{min}. These points are represented by ○ and △ in Fig. 19, respectively.

The *h/t* ratio which gives the minimum stiffness ratio, γ^U_{min}, against the ultimate strength of a one-sided stiffened plate may be approximated by the intersecting point of the overall buckling strength curve and the ultimate strength curve for Mode *LL* collapse, which are expressed by the following equations[16,18-20].

Overall buckling strength:

$$\sigma_{cr}/\sigma_Y = [(N+1)\gamma_e + \{1+(a/b)^2\}^2]\pi^2 D / [\alpha^2 t\{1+(N+1)\delta\}\sigma_Y] \quad (15)$$

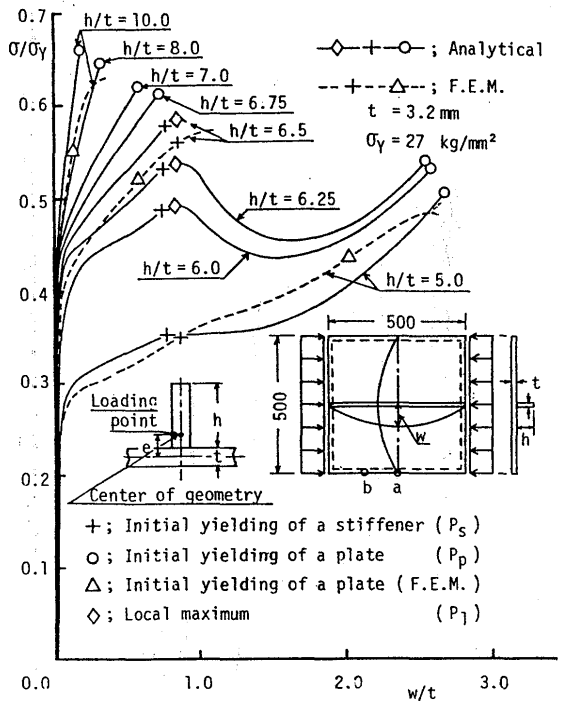

Fig.17 Average stress-deflection curves for one-sided stiffened plates under compression

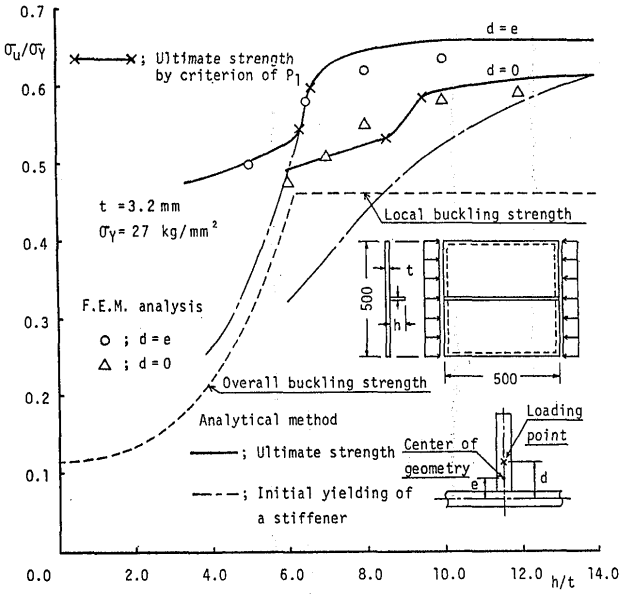

Fig.18 Ultimate strength of one-sided stiffened plate under compression

Local collapse strength:

$$\sigma_u/\sigma_Y=[\sigma_{up}/\sigma_Y+N\delta\,\sigma_{us}/\sigma_Y]/(1+N\delta) \qquad (16)$$

where N, σ_{up} and σ_{us} are the number of stiffeners, ultimate strength of a plate and a stiffener, respectively, and

$$\gamma_e=E[I_s+ht_sc^2\{1-8N\delta/\pi^2(1+N\delta)\}]/bD$$
$$c=(h+t)/2,\quad I_s=t_sh^3/12,\quad D=Et^3/12(1-\nu^2),$$
$$\delta=ht_s/bt$$

In Fig. 19, N was taken as 1.

The point giving the approximate minmum stiffness ratio by these equations is indicated by ● in Fig. 19. It should be noted that the maximum value of the ultimate strength is not attained by the minimum stiffness ratio in the case of a one-sided stiffened plate. It seems that the stiffener of which stiffness ratio is about 3.5 times of γ^U_{min} is necessary to attain the maximum limiting value of the ultimate strength of a one-sided stiffened plate.

Figure 20 shows the influence of welding residual stresses on the ultimate strength of a one-sided stiffened plate[16]. The same type of distribution of welding residual stresses was assumed as in the case of both-sided stiffened plates in the analysis. Comparing the ultimate strengths in Fig. 20 with those in Fig. 19, it is observed that the welding residual stresses increase the ultimate strengths in an overall mode, but reduces those in a local mode.

For the plate of which aspect ratio is 0.5, the ultimate strength was evaluated by the same method changing the number of stiffeners from three to six[16,18-20]. The initial deflection of $A_o/t = B_o/t = 0.01$ was assumed in the analysis. The calculated ultimate strengths are plotted in **Fig. 21** by solid lines. The dashed lines in Fig. 21 represent the buckling strength by Eq. (15) and the chain lines the ultimate strength by Eq. (16).

When collapse of Mode *LO* takes place, the ultimate strength was approximated with the buckling strength evaluated by Eq. (15) assuming that local buckling does not occur when the magnitude of initial deflection is small. In this case, the ultimate strength in Mode *LL* was also approximated by Eq. (16) in good accuracy.

The ultimate strength of a girder of I-section under pure bending was also discussed in Ref. 17) when a horizontal stiffener was attached to its web plate, and a simple method was proposed to predict the ultimate strength and the minimum stiffness ratio against the ultimate strength.

5. Conclusions

In this paper, the fundamental behaviors of compressed plates and stiffened plates and influences of welding residual stresses and initial deflection on them have been described based on the theoretical and experimental investigations. The results are summarized as follows.

(1) When the plate is long and thin, a large deflection is produced before yielding takes place. Above the

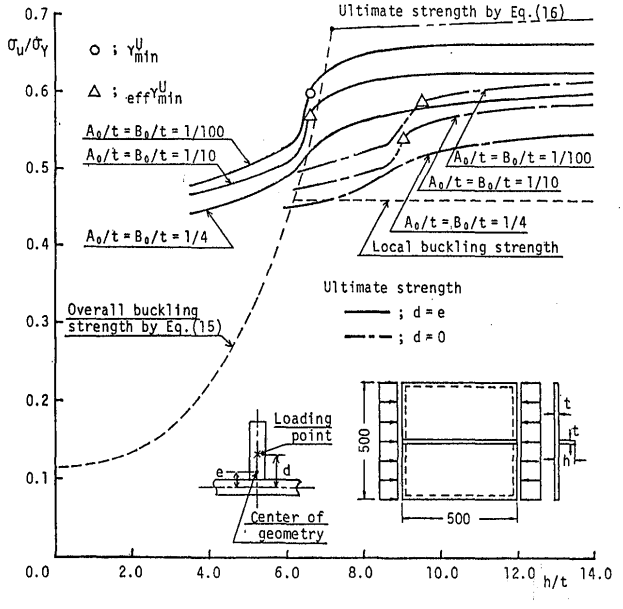

Fig.19 Influence of initial deflection on compressive ultimate strength of one-sided stiffened plates

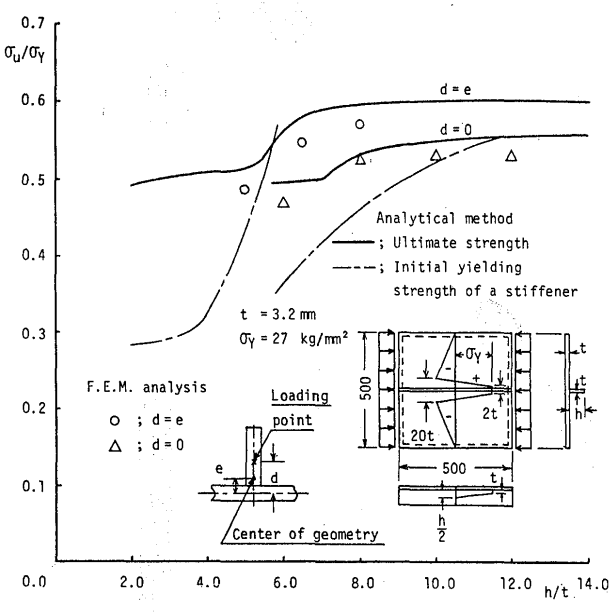

Fig.20 Influence of welding residual stresses on compressive ultimate strength of one-sided stiffened plates

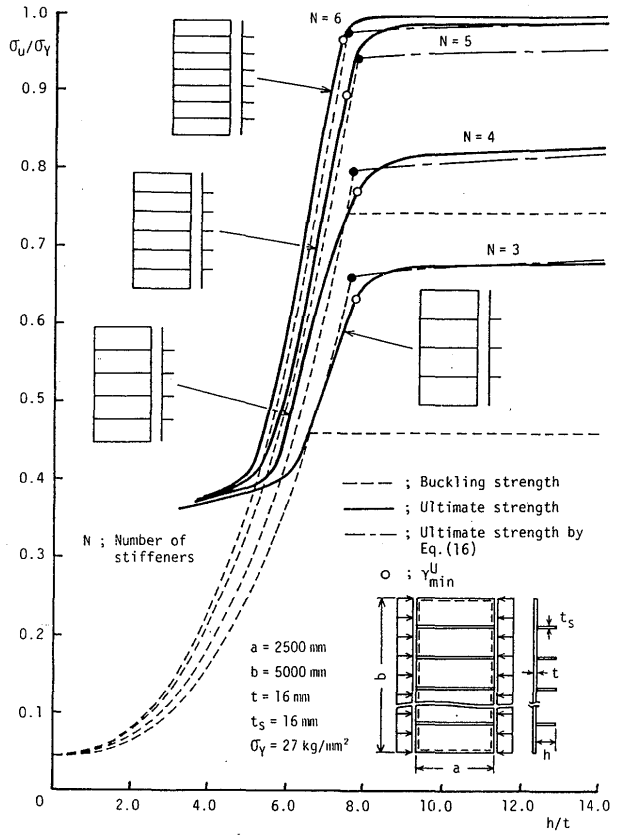

Fig.21 Compressive ultimate strength of one-sided multi-stiffened plates

buckling load, only one mode component of the initial deflection is amplified and becomes stable as the load increases. This stable mode is not necessarily the buckling mode, but is usually one or two modes higher. Only the component of the stable deflection mode influences the ultimate strength. The magnitude of this component in the initial deflection is usually significantly smaller than the maximum initial deflection.

(2) In the case of a long thick plate in compression, the largest curvature of initial deflection is a main cause to initiate the spread of plastic zone in the plate, which results in loosing the carrying capacity and leading to collapse. The maximum curvature is more influential upon reduction of the ultimate strength than maximum magnitude of initial deflection.

(3) Both welding residual stresses and initial deflection reduce the compressive buckling and ultimate strengths of plates. The reduction in ultimate strength is maximum when $(b/t)\sqrt{\sigma_Y/E}$ is about 1.8.

(4) When the stiffener is symmetric with respect to the middle plane of the plate, the secondary buckling in an overall mode takes place after the primary buckling in a local mode has occurred in the range of stiffness ratio greater than GBin.

(5) There exist three typical collapse modes of stiffened plates according to the stiffness ratio of the stiffener to the plate, which are: (a) Mode *OO* (overall collapse after overall buckling); (b) Mode *LO* (overall collapse after local buckling) and (c) Mode *LL* (local collapse after local buckling).

(6) Welding residual stresses reduce the compressive buckling and ultimate strengths of stiffened plates when local buckling takes place, but increase them when overall buckling occurs. Initial deflection both in the plate and the stiffeners reduce the compressive ultimate strength of stiffened plates.

(7) For symmetrically both-sided stiffened plate, it is found and confirmed that there exist two significant stiffness ratios, γ^U_{low} and γ^U_{min}, of a stiffener to the plate against the compressive ultimate strength. Among these, γ^U_{min} is especially important since it is the minimum required value of the stiffness ratio which guarantees that the stiffened plate reaches its maximum limiting ultimate strength. It has the same meaning as the minimum stiffness ratio, γ^B_{min}, against the buckling strength.

(8) For the one-sided stiffened plate, the minimum stiffness ratio, γ^U_{min}, can also be determined as defined for both-sided stiffened plates. However, about 3.5 times of the stiffness ratio of γ^U_{min} is necessary to attain the maximum limiting value of ultimate strength.

(9) When stiffened plates are accompanied by initial deflection or the load is applied eccentrically, the effective minimum stiffness ratio, ${}_{eff}\gamma^U_{min}$, against the ultimate strength may be defined, which has the same physical meaning as γ^U_{min}.

(10) Both initial deflection and welding residual stresses reduce the minimum stiffness ratios, γ^B_{min} and γ^U_{min}, as well as the maximum limiting value of buckling and ultimate strengths which are guaranteed by these stiffness ratios.

References

1) Ueda, Y. and Tall, L.: "Inelastic Buckling of Plates with Residual Stresses," IABSE, Zurich (1967), pp211-254.
2) Nishino, N., Ueda, Y. and Tall L.: "Experimental Investigation of the Buckling of plates with Residual Stresses", Special Technical Publication, No.419, ASTM (1966), pp.12-30.
3) Ueda, Y., Yasukawa, W. and Uenishi, M.: "Inelastic Local Buckling of Built-Up I-Section", Reports of the Osaka Univ., Vol.16, No.737 (1966), pp.643-656.
4) Ueda, Y., Yasukawa, W., Yao, T., Ikegami, H. and Ohminami, R.: "Effect of Welding Residual Stresses and Initial Deflection on Rigidity and Strength of Square plates Subjected to Compression (Report 1)", J. Soc. Naval Arch.

of Japan, Vol.137 (1975), pp.315-326 (in Japanese), and Trans. JWRI (Japan Welding Research Institute, Osaka Univ.), Vol.4, No.2 (1975), pp.29-43.
5) Ueda, Y., Yasukawa, W., Yao, T., Ikegami, H. and Ohminami, R.: "Effect of Welding Residual Stresses and Initial Deflection on Rigidity and Strength of Square plates Subjected to Compression (Report 2)", J. Soc. Naval Arch. of Japan, Vol.140 (1976), pp.205-209 (in Japanese), and Trans. JWRI, Vol.6, No.1 (1977), pp.29-43.
6) The Society of Naval Arch. of Japan: "Japan Shipbuilding Quality Standards", (1975), Tokyo.
7) Institute de Recherches de la Construction Navale: "Standards de Quality Coque Metallique", (1976), Paris.
8) Ueda, Y. and Yao, T.: "Ultimate Strength of a Rectangular Plate under Thrust - with Consideration of the Effects of Initial Imperfections due to Welding -", Trans. JWRI, Vol.8, No.2 (1979), pp.97-104.
9) Ueda, Y., Yao, T. and Nakamura, K.: "Compressive Ultimate Strength of Rectangular Plates with Initial Imperfections due to Welding - Effects of the Shape and Magnitude of Initial Deflection -", J. Soc. Naval Arch. of Japan, Vol.148 (1980), pp.222-231 (in Japanese).
10) Ueda, Y. and Yao, T.: "Compressive Ultimate Strength of Rectangular Plates with Initial Imperfections due to Welding - Effects of Initial Deflection and Welding Residual Stresses -", J. Soc. Naval Arch. of Japan, Vol.149 (1981), pp.306-313 (in Japanese).
11) Ueda, Y., Yao, T., Nakacho, K., Tanaka, Y. and Handa, K.: "Compressive Ultimate Strength of Rectangrlar Plates with Initial Imperfections due to Welding - Prediction Method of Compressive Ultimate Strength -", J. Soc. Naval Arch. of Japan, Vol.154 (1983), pp.345-355 (in Japanese).
12) Ueda, Y., Nakacho, K. and Moriyama, S.: "Compressive Ultimate Strength of Rectangular Plates with Initial Imperfections due to Welding - Prediction Method for Initial Imperfection, Effective Coefficient of Initial Deflection and Compressive Ultimate Strength -", J. Soc. Naval Arch. of Japan, Vol.159 (1986), pp.283-294 (in Japanese).
13) Ueda, Y. and Yao, T.: "The Influence of Complex Initial Deflectition Modes on the Behaviour and Ultimate Strength of Rectangular Plate in Compression", J. Constructional Steel Research, Vol.5 (1985), pp.265-302.
14) Ueda, Y., Yao, T. and Kikumoto, H.: "Minimum Stiffness Ratio of a Stiffener against Ultimate Strength of a Stiffened Plate", J. Soc. Naval Arch. of Japan, Vol.139 (1976), pp.199-204 (in Japanese).
15) Ueda, Y., Yao, T., Katayama, M. and Nakamine, M.: "Minimum Stiffness Ratio of a Stiffener against Ultimate Strength of a Stiffened Plate (2nd Report)", J. Soc. Naval Arch. of Japan, Vol.143 (1978), pp.308-315 (in Japanese).
16) Ueda, Y., Yao, T., Nakamine, M. and Nakamura, K.: "Minimum Stiffness Ratio of a Stiffener against Ultimate Strength of a Stiffened Plate (3rd Report)", J. Soc. Naval Arch. of Japan, Vol.145 (1979), pp.176-185 (in Japanese).
17) Ueda, Y., Yao, T. and Fujikubo, M.: "Minimum Stiffness Ratio of a Stiffener against Ultimate Strength of a Stiffened Plate (4th Report)", J. Soc. Naval Arch. of Japan, Vol.148 (1980), pp.252-260 (in Japanese).
18) Ueda, Y. and Yao, T.: "Ultimate Strength Stiffened plates and Minimum Stiffness Ratio of Their Stiffeners (under Thrust)", Trans. JWRI, Vol.10, No.2 (1981), pp.97-109.
19) Ueda, Y. and Yao, T.: "Ultimate Strength of Stiffened Plates and Minimum Stiffness Ratio of Their Stiffeners", Naval Arch. and Ocean Engineer, Vol.19 (1981), pp.133-156.
20) Ueda, Y. and Yao, T.: "Ultimate Strength of Compressed Stiffened Plates and Minimum Stiffness Ratio of Their Stiffeners", J. Eng. Struct., Vol.5, No.4 (1983), pp.97-107.